

HYDROGEN EFFECT ON FATIGUE AND FRACTURE RESISTANCE OF A PIPE STEEL UTICAJ VODONIKA NA OTPORNOST PREMA ZAMORU I LOMU ČELIKA ZA CEVI

Originalni naučni rad / Original scientific paper
UDK /UDC: 621.643.027:669.15:539.431
620.17:669.15
Rad primljen / Paper received: 25.01.2009

Adresa autora / Author's address:

¹) Laboratoire de Fiabilité Mécanique - Ecole Nationale
d'Ingénieurs de Metz et Université Paul Verlaine Metz, Ile
du Saulcy, Metz, France, j.capelle@enim.fr

²) Karpenko Physico-Mechanical Institute of National
Academy of Sciences of Ukraine, Lviv, Ukraine

Keywords

- hydrogen
- API 5L X52
- fracture toughness
- Wöhler curve
- "Roman Tile" specimen

Abstract

Transport by pipelines is more used at the present time to transfer liquid or gas sources of energy from the location of extraction to the region of use. With the reduction of oil reserves, hydrogen became an interesting source of energy. To avoid any risk of explosion or escape during hydrogen transport and to reduce the problem of pollution and fatal consequences, mechanical properties of steels used for the manufacturing of pipes should be known. In the paper the results of experimental analyses of the hydrogen effect on mechanical properties of API 5L X52 pipe steel regarding its resistance to fatigue and fracture are presented.

INTRODUCTION

The European gas pipelines network plays very important role for national economies. The importance will permanently increase with prospective plans of introducing European hydrogen energy infrastructure, /1, 2/, and due to the use of existing pipelines network for transportation of natural gas and hydrogen mixtures. Within the European project NATURALHY, 39 European partners have joined efforts to be prepared for the hydrogen economy and to assess the development of hydrogen as an energy carrier in existing gas network, /3/. Experiments presented in this paper had been performed within Work Package 3 (WP3): Durability, Task 3.2 (Transmission pipelines). Key issues are durability of pipeline material, safety, integrity management, life cycle and social-economical aspects. The nature of gas pipeline failures are different, Fig. 1. They can appear by fracture or by leakage, depending on the properties of transported fluid. The majority of failures are caused by pitting corrosion or stress corrosion cracking, and many problems are related to welding defects. Movement of ground (landslip, earthquake) can also cause damage of buried pipelines. The owners of pipelines have studied these problems and have impressive experience and had developed methods enabling to manage the problem.

Ključne reči

- vodonik
- API 5L X52
- žilavost loma
- Velerova kriva
- epruveta "rimski crep"

Izvod

Transport cevima se u novije vreme sve više koristi za prenos tečnih ili gasovitih izvora energije od mesta dobijanja do područja njihove upotrebe. Sa smanjenjem rezervi nafte vodonik postaje interesantan izvor energije. Da bi se izbegao bilo kakav rizik od eksplozije ili isticanja vodonika tokom transporta i smanjio problem zagađivanja i kobnih posledica, treba poznavati mehaničke osobine čelika koji se koriste za izradu cevi. U radu su prikazani rezultati eksperimentalne analize uticaja vodonika na mehaničke osobine čelika API 5L X52 za cevi u pogledu njegove otpornosti prema zamoru i lomu.

External mechanical damages should not be neglected, Fig. 1. Pipelines can be accidentally damaged or broken during excavation operation of ground moving machines. Crack initiation by fatigue and fracture emanating from stress concentrations are the origin in 90% of service failure cases. The presence of a geometrical discontinuity like notch will reduce the fracture resistance of the pipeline material. Due to reduced cross-section area of the pipe wall, it becomes more sensitive to the operating pressure and the loading caused by the movements of ground, since local stress increases exponentially with defect size.

This study is devoted to corrosion failures emanating from notches during the lifespan of analysed pipelines, since they present 42% of total failures (Fig. 1).

FRACTURE TOUGHNESS

The electrolytic solution for hydrogen charging is used in the experiment to achieve a strong concentration in hydrogen ion in the vicinity of mechanical notch. Synthetic solution NS4 (Natural Soil 4) represents the ground around pipelines where corrosion is observed all over the world.

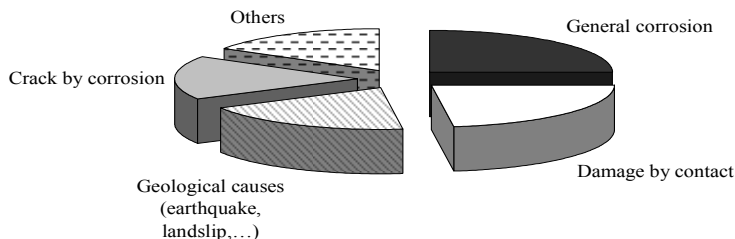


Figure 1. Causes of the fracture of pipelines in the course of exploitation recorded by the members of the ACPRÉ from 1985 to 1995, /4/.
Slika 1. Uzroci loma cevovoda tokom eksploatacije evidentirani od strane članova ACPRÉ od 1985 do 1995, /4/

Solution preparation for hydrogenisation

The NS4 solution of standard composition, Table 1, with original pH value between 8 and 8.5, was prepared in a volume of 17 litres from given chemical compounds, distilled and deionised water. A pump is used to save solution homogeneity during fatigue test. During the first test, pH value of 8.56 was measured. To decrease the pH value to 6.7, as requested for fatigue test, the bubbling of the gas mixture (80% N₂ and 20% CO₂) had been applied to stabilize the solution and to remove the oxygen. The level of pH value was held between 6.6 and 6.7 during the test.

Table 1. Chemical compound of the NS4 solution, /5/.
Tabela 1. Hemijski sastav NS4 rastvora, /5/

Chemical compound	Formula	Concentration, mg/l
Potassium chloride	KCl	122
Sodium hydrogen carbonate	NaHCO ₃	483
Hydrated calcium chloride	CaCl ₂ ·2H ₂ O	181
Hydrated magnesium sulphate	MgSO ₄ ·7H ₂ O	131

Specimens were charged by hydrogen at constant polarisation potential of $E_p = -1$ V (SCE). This value is slightly more negative than free corrosion potential for given steel ($E_{corr} = -0.8$ V (SCE)). In this experimental procedure the potentiostat VMP, /6/, had been used.

Testing of fracture mechanics parameters

Compact Tensile test (CT) specimen according to French standards NF A 03-180, /7/, and NF A 03-182, /8/, had been used in the experiment (Fig. 2). Specimens were prepared from pipe samples, having the pre-crack in longitudinal direction of the pipe. The dimensions of specimens were:

$L_t = 120$ mm, $L = 55$ mm, $D = 20$ mm, $B = 10$ mm
 $W = 100$ mm, $W_t = 125$ mm, $e = 5$ mm, $h = 46$ mm.

Four specimens were tested, two for reference test in air at room temperature, and two for the test in solution for hydrogen charging. The specimen had been exposed to load of sinusoidal shape at frequency of 15 Hz, maximum load 7500 N, and 0.1 load ratio, in order to obtain fatigue pre-crack of initial length $a_0 = 9$ mm. The exposition to solution for hydrogenisation was performed with no mechanical load. Electrolysis lasted 7 days at constant potential, -1 V (SCE). Tests were carried out in displacement control, with the rate of 0.02 mm/s. Test results are given in Fig. 3 and Table 2 for non pre-treated specimens and specimens exposed to solution for hydrogenisation before test.

The clip gauge was used to measure notch opening displacement at distance z from the load-line on the front face of straight-notch and produced pre-crack.

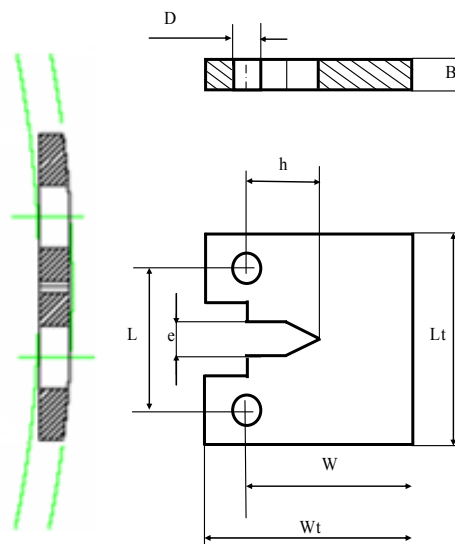


Figure 2. CT specimen (geometry and location in the pipe wall).
Slika 2. CT epruveta (geometrija i položaj u zidu cevi)

In the performed tests it was not possible to obtain critical stress intensity factor (plane strain fracture toughness), K_{Ic} value, since the thickness of specimens was not sufficient for this ductile steel. So, crack-tip opening displacement, δ_i , and stress intensity factor (fracture toughness) at the initiation, K_{Ii} , were determined.

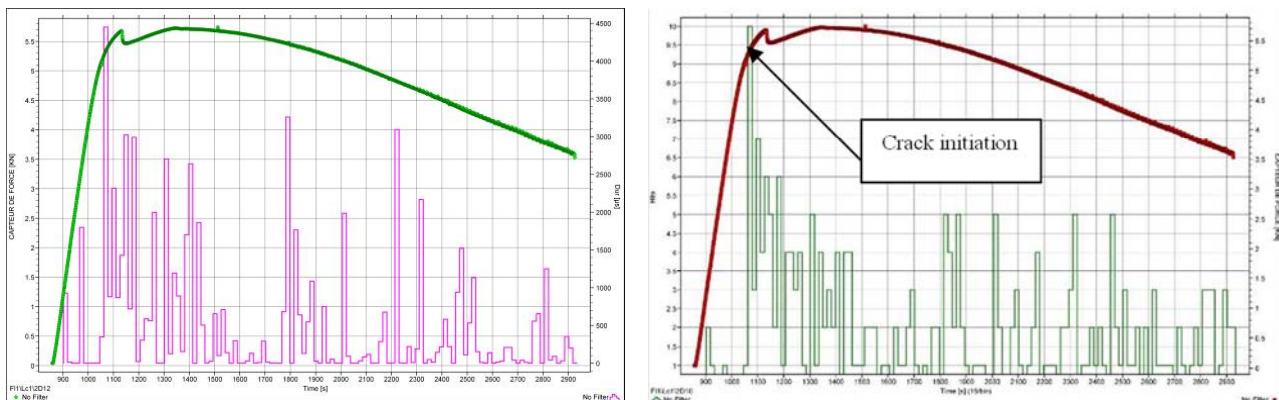
They are calculated according to French standards, /7, 8/:

$$\delta_i = \frac{K_{Ii}^2 (1 - \nu^2)}{2R_{p0,2}} + \frac{0,4(W - a_0)}{(0,4W + 0,6a_0 + z)} \nu_p \quad (1)$$

$$K_{Ii} = \frac{F_i}{BW^{1/2}} f\left(\frac{a_0}{W}\right) \quad (2)$$

Crack initiation was detected by acoustic emission. The correspondence in time between load level and acoustic emission signal, presented in Fig. 3, indicated critical moment for crack initiation, close to “pop-in”. Acoustic events of the highest duration and the most important number of acoustic hits are easily detectable.

Results of fracture mechanics parameters testing, expressed in values of stress intensity factor (SIF) and crack tip opening displacement (CTOD), are presented in Table 2. According to these results, one can conclude that hydrogen content has an influence on crack initiation, expressed by 13% decrease of SIF at initiation, but its effect on the maximum SIF is negligible. A more significant result is found for CTOD, δ_i , with a decrease of 49%.



a) non pre-treated specimen
 a) nepripremljena epruveta
 b) specimen exposed to solution for hydrogenisation
 b) epruveta izložena rastvoru za zasićenje vodonikom

Figure 3. Tensile and acoustic emission signal testing: time dependence on load, acoustic emission duration and recorded hits.
 Slika 3. Ispitivanje zatezanjem i akustičnom emisijom: vremenska zavisnost sile, trajanja akustične emisije i zabeleženi signali

Table 2. Fracture toughness, K_I , and crack mouth opening displacement, δ_i , values in pipe longitudinal direction, steel API 5L X52.
 Tabela 2. Žilavost loma, K_I , i otvaranje usana prsline, δ_i , vrednosti u uzdužnom pravcu cevi, čelik API 5L X52

Environment	Specimen	Stress intensity factor (Fracture toughness), $MPa\sqrt{m}$				Crack tip opening displacement, CTOD, mm	
		at initiation		maximum		δ_i	average, δ_i , mean
		K_{Ii}	average, K_{Ii} , mean	K_{Imax}	average, K_{Imax} , mean		
Air	CT1-A	97.59	95.54	108.02	109.60	0.21	0.175
	CT2-A	93.49		111.19		0.14	
Hydrogen solution	CT1-H	85.55	82.69	111.49	109.71	0.10	0.09
	CT2-H	79.84		107.93		0.08	
Difference			-13.44%		0.1%		-48.61

Testing of curved specimen, taken from the pipe wall

In order to simulate the real situation of mechanically damaged pipes by scratches, notches or gouges, curved specimens, known as “Roman tile” type (Fig. 4), are taken from available pipes, produced of steel API 5L X52. Due to the small thickness and the important curvature of the pipe, it was not possible to design convenient standard specimen, as single-edge notched bend (SEN-B) specimen. So, the specimen was of thickness $t = 11$ mm, width $b = 40$ mm, and length corresponding to segment of central angle of $\theta = 70^\circ$ and diameter $D = 610$ mm. Specimens were made with machined V notch on an outer surface along the width, $0.2t$ deep, at angle 45° , rounded at the root by $r = 0.15$ mm, in a longitudinal pipe direction, simulating the expected scratch damage (Fig. 5).

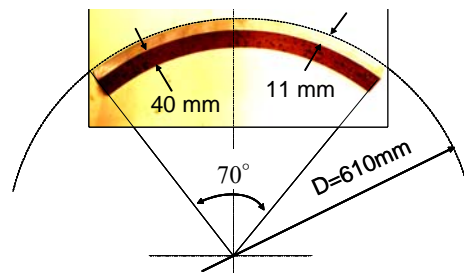


Figure 4. “Roman tile” specimen.
 Slika 4. Epruveta “rimski crep”

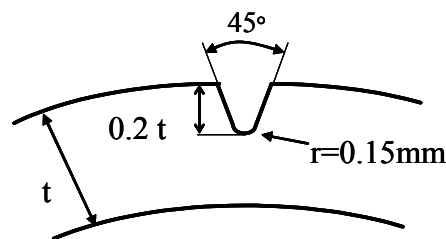


Figure 5. Notch geometry.
 Slika 5. Geometrija zarez

The longitudinal position of a notch corresponds to the maximum stress acting in the pipeline. However, by testing V notched “Roman tile” type specimen it was not possible to determine standardised fracture toughness, only the data about notch fracture toughness of damaged pipe could be obtained. These data are very useful to evaluate fracture resistance of damaged pipes, having in mind that they were also tested in aggressive environment of NS4 solution.

Special testing device was necessary for positioning of the specimen (Fig. 6). The bend-test fixture was positioned on the closed loop hydraulic testing machine with a load cell of capacity ± 10 kN. The specimen was loaded in three-point bending through a support A and supporting rollers B and C. Support and rollers were produced from polyvinyl chloride (PVC) to reduce friction.

All tests had been performed under quasi-static loading in displacement control. Displacement rate was monitored during the test in order to assure the value of 0.01 mm/s. The individual test lasted about 30 minutes.

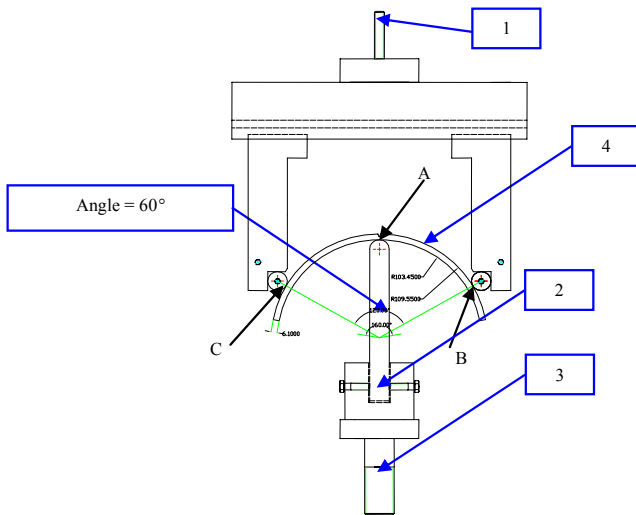


Figure 6. "Roman tile" specimen fixture and testing assembly
 1-connection with load cell; 2-transmitting component with rounded tip; 3-connection of test assembly with the testing machine bottom; 4-"Roman tile" specimen.

Slika 6. Sistem postavljanja za ispitivanje epruvete "rimski crep"
 1-spoj sa jedinicom za opterećivanje; 2-komponenta sa zaobljenim vrhom za prenos sile; 3-spoj sistema za ispitivanje sa donjim delom kidalice; 4-epruveta "rimski crep"

Fracture toughness of notched specimens, K_{pi}

Due to the shape of selected specimen it was not possible to produce proper fatigue pre-crack. Instead, V notch is selected (Fig. 5) for fracture testing. In this case fracture toughness, $K_{\rho,c}$, depends on notch radius size, /9/. It is well known that the critical stress intensity factor (plane strain fracture toughness) K_{Ic} can be obtained only when notch root radius ρ is smaller than the critical value, ρ_{cr} :

$$K_{\rho,c} = K_{Ic} \quad \text{for} \quad \rho < \rho_{cr} \quad (3)$$

and for this fatigue pre-crack the condition for valid K_{Ic} measurement is fulfilled together with specimen thickness. This condition is not fulfilled here, since actual notch root radius is larger than critical ($\rho > \rho_{cr}$), and only fracture toughness (stress intensity factor), $K_{\rho,c}$, proportional to $\sqrt{\rho}$ can be measured in this situation

$$K_{\rho,c} =: \sqrt{\rho} \quad \text{for} \quad \rho \geq \rho_{cr} \quad (4)$$

The increase of fracture toughness with notch radius is a consequence of increased plastic zone size ahead of notch root (Fig. 7) for larger root radius and for the required increase of consumed total work for fracture. The critical notch radius can be determined from the volume of fracture process zone since it corresponds to the volume of plastic zone ahead of notch root, /10/. It is reasonable to measure the fracture toughness of the specimen with representative notch root radius. With this in mind, as representative for a severe notch type defect the notch radius $\rho = 0.15$ mm is selected, sufficiently conservative to produce acceptable results. Compared with other low strength steels this root radius value is probably even lower than the critical notch root radius value.

The concept of critical notch stress intensity factor and corresponding local fracture criterion assumes that the frac-

ture process will take place in a volume of certain determined size, /9/. This local fracture approach is called the Volumetric Method (VM). The process zone volume is assumed to be a cylinder of diameter known as the effective distance. Determination of effective distance is based on bi-logarithmic elastic-plastic stress distribution (Fig. 7), originating at notch root front because the fracture process zone is the highest stressed zone. This zone is characterized by an inflexion point in the stress distribution at the transition from zone II to III (Fig. 7).

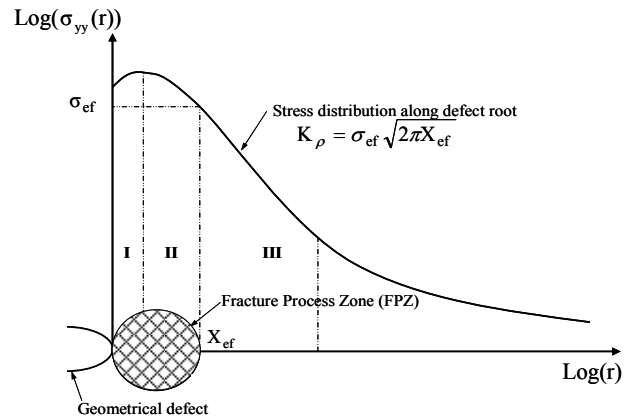


Figure 7. Schematic distribution of elastic-plastic stress ahead of notch tip in the plane of fracture extension and the concept of notch stress intensity.

Slika 7. Shematski prikaz raspodele elasto-plastičnog napona ispred vrha zarezu u ravni razvoja loma i koncept intenziteta napona zarezu

Effective stress can be calculated from the expression:

$$\sigma_{eff} = \frac{1}{X_{eff}} \int_0^{X_{eff}} \sigma_{yy}(r) \Phi(r) dr \quad (5)$$

Here, σ_{ef} , X_{ef} , $\sigma_{yy}(r)$, and $\Phi(r)$ are effective stress, effective distance, opening stress and weight function, respectively. The stress distribution is corrected by a weight function in order to take into account the distance from notch tip of the acting point and the stress gradient at this point. The effective distance corresponds to the inflexion point with the minimum of the relative stress gradient χ , which can be written as:

$$\chi(r) = \frac{1}{\sigma_{yy}(r)} \frac{\partial \sigma_{yy}(r)}{\partial r} \quad (6)$$

The effective stress is considered as the average value of the stress distribution within the fracture process zone.

The notch stress intensity factor is defined as a function of effective distance and effective stress, /9/:

$$K_{\rho} = \sigma_{ef} \sqrt{2\pi X_{ef}} \quad (7)$$

and describes the stress distribution in zone III as given by the following equation:

$$\sigma_{yy} = \frac{K_{\rho}}{(2\pi r)^{\alpha}} \quad (8)$$

where K_{ρ} is the notch intensity factor, α is the exponent of the power function of stress distribution, of a constant

value. Failure occurs when the notch stress intensity factor K_{ρ} reaches critical value, i.e. the notch fracture toughness $K_{\rho,c}$, which is a measure of the resistance to fracture initiation from the notch tip.

The stress distribution ahead of the notch tip and along the ligament in notch plane is computed by finite elements for critical load defined by acoustic emission technique. The critical notch stress intensity factor $K_{\rho,c}$ is calculated using the effective distance and effective stress obtained from the relative stress gradient, as presented in Fig. 8.

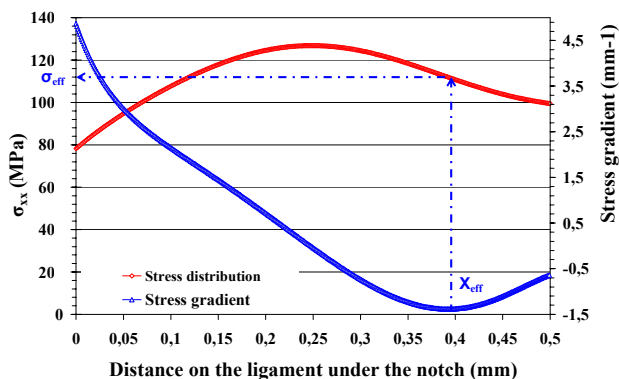


Figure 8. Determination of effective distance using the relative stress gradient method.

Slika 8. Određivanje efektivnog rastojanja primenom metode gradijenta napona

The fracture toughness value is given at fracture initiation, detected in the same way as for CT specimen. The obtained results are presented in Table 3.

Table 3. Critical notch stress intensity factor $K_{\rho,i}$ at fracture initiation of “Roman tile” type specimen—testing in air.

Tabela 3. Kritični faktor intenziteta zareza $K_{\rho,i}$ pri inicijaciji loma epruvete “rimski crep”—ispitivanje na vazduhu

Specimen	1	2	3	4	5	6	7	8	
Critical load	N	9300	8300	9350	9180	8710	9350	10120	8850
$K_{\rho,i}$	MPa√m	96.77	62.99	70.35	68.08	65.45	70.53	79.12	66.51
Mean critical load, N							9145		
Standard deviation, N							541.19		
Mean $K_{\rho,i}$, MPa√m							69.25		
Standard deviation, MPa√m							4.81		

The mean value of notch fracture toughness $K_{\rho,c}$ in air is 69.25 MPa√m, with standard deviation 4.81 MPa√m.

In order to analyze the effect of aggressive environment, the same tests have been performed with specimens exposed to electrolytic hydrogen, for different exposition times. Obtained results of time dependence of critical notch stress intensity factor $K_{\rho,i}$ at initiation are presented in Fig. 9. Each point on the diagram presents the mean value of two tests. After 700 hours of exposition to solution for hydrogenisation, the notch stress intensity factor is reduced by 25% to the value of 51.94 MPa√m.

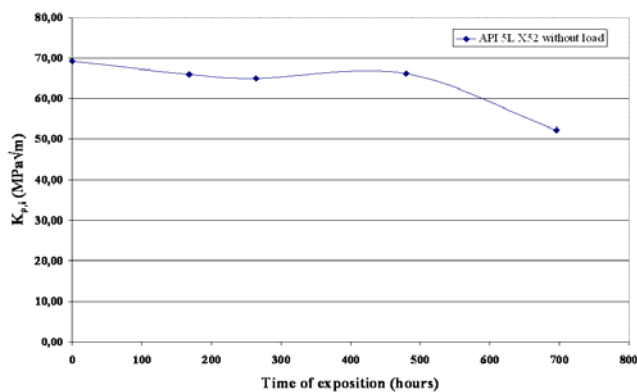


Figure 9. Evolution of notch fracture toughness at initiation $K_{\rho,i}$ with exposition time.

Slika 9. Promena žilavosti loma zareza pri inicijaciji $K_{\rho,i}$ sa vremenom ispitivanja

FATIGUE TEST

Fatigue tests had been performed in order to obtain more data about detrimental effect of ground environment on the resistance of steel.

Fatigue test procedure

Closed loop hydraulic testing machine with a load cell of capacity ±10 kN was used for fatigue test of “Roman tile” specimens applied in this experiment. The testing machine in operation with bend-test fixture, similar to the fixture for static test, and the test set-up for three-point bend test of “Roman tile” specimens are presented in Fig. 10.

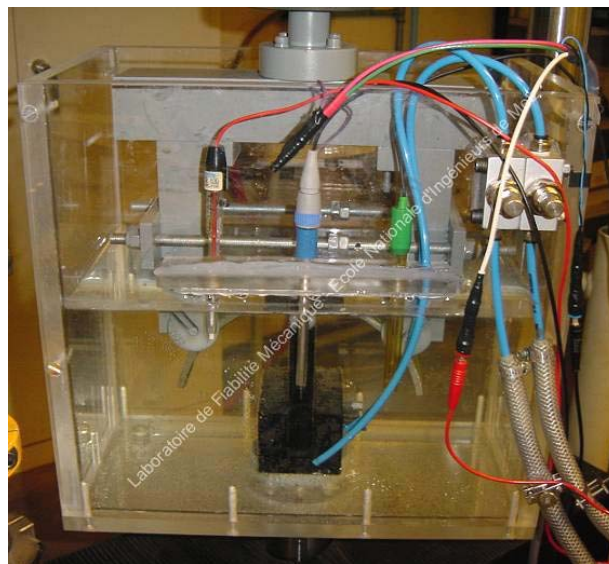


Figure 10. Device for “Roman tile” specimen testing in hydrogen environment.

Slika 10. Uređaj za ispitivanje epruveta “rimski crep” u atmosferi vodonika

The applied load, frequency and sinusoidal fatigue cycle were monitored during the test on control panel. Hydrogen charging was performed using the same cell as in static test, filled with NS4 solution. Test conditions are listed in Table 4. It is to accentuate that selected and set load ratio in the experiment was 0.5, slightly different from that experienced in the service condition, when it was 0.57.

Table 4. Fatigue test conditions.
Tabela 4. Uslovi zamornog ispitivanja

Form of the cycle	Sinus
Frequency	0.05 Hz
Selected load ratio	0.5
Working potential	-1 V (SCE)
Electrolytic solution	Natural Soil 4 (NS4)
Solution pH	Controlled between 6.66 and 6.74

Crack initiation was detected by acoustic emission and Wöhler curves were drawn for both initiation and fracture

values. The classical power fit is in accordance with Basquin's law:

$$\Delta\sigma = \sigma_f (N_R)^b \tag{9}$$

where σ_f stands for fatigue resistance and b the Basquin's exponent.

Results

Two sets of fatigue tests were performed, in air and in NS4 solution. Results were analysed for the initiation and final fracture, as presented by Wöhler curves in Fig. 11.

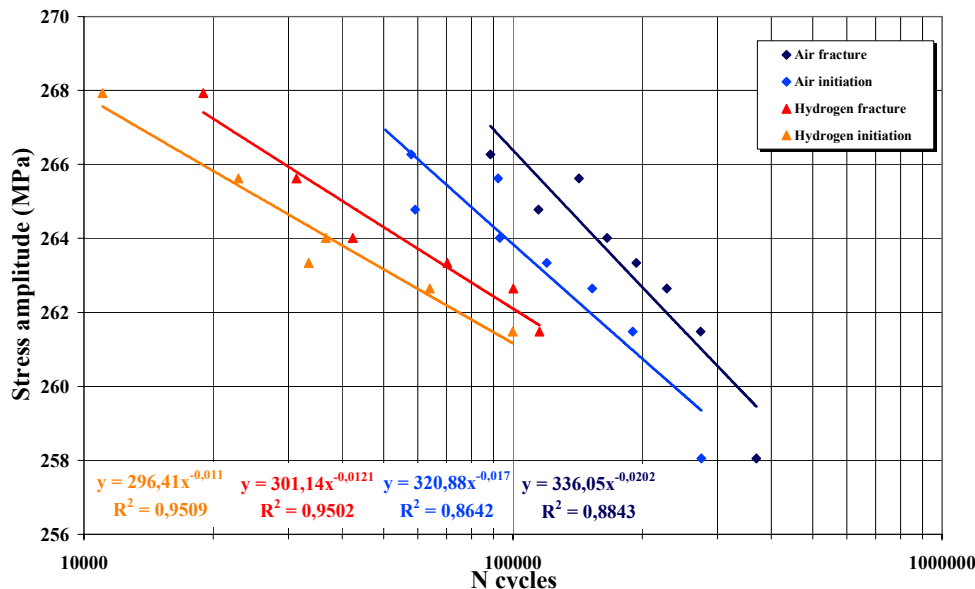


Figure 11. Wöhler curves.
Slika 11. Velerove krive

Results are presented in bi-logarithmic coordinates of stress amplitude vs. number of cycles, Fig. 11. Two Wöhler curves are presented, for both the air and hydrogen environment, the first one being classic, at fracture, and the second at initiation.

An important reduced life is found for tests performed in hydrogen solution, 68% in average. Wöhler curves at initiation confirmed the hydrogen effect, found in static tests. Crack initiation represents 62% of the life duration in air, 78% in the hydrogen environment. The hydrogen effect on crack propagation cannot be neglected.

REFERENCES

1. Fernandes, T.R.C., da Graça Carvalho, F.C., "HySociety" in support of European hydrogen projects and EC policy. International Journal of Hydrogen Energy, 30 (2005), 239-245.
2. Mulder, G., Hetland, J., Lenaers, G., Towards a sustainable hydrogen economy: Hydrogen pathways and infrastructure, International Journal of Hydrogen Energy, 32, Issues 10-11 (2007), 1324-1331.
3. NaturalHy Project, <http://www.naturalhy.net>
4. Rapport de l'enquête MH-2-95, Fissuration par corrosion sous tension des oléoducs et des gazoducs canadiens, Office National d'Énergie, (1996)
5. Capelle, J., Gilgert, J., Dmytrakh, I., Pluvinaige, G., Sensitivity of pipelines with steel API X52 to hydrogen embrittlement,

CONCLUSION

Results of fracture tests have shown different effects of hydrogen on fracture toughness, a small decrease when expressed by stress intensity factor and a much higher decrease expressed in the crack-tip opening displacement. The effect of hydrogen is confirmed by fatigue tests, expressed by a reduced life of 68%. In addition, hydrogen effect is more pronounced by increasing stress.

- International Journal of Hydrogen Energy, 33, Issue 24, (2008), 7630-7641.
6. Potentiostat VMP, Manual, Princeton Applied Research, 2004.
7. NF A 03-180, Détermination du facteur d'intensité de contrainte critique des aciers, Afnor, (1981).
8. NF A 03-182, Détermination de l'écartement à fond de fissure (CTOD), Afnor, (1987).
9. Pluvinaige, G., Fracture and fatigue emanating from stress concentrators, Kluwer (2003).
10. Akourri, O., Louah, M., Kifani, A., Gilgert, G., Pluvinaige, G., The effect of notch radius on fracture toughness J_{Ic} , Eng Fract Mech 65 (2000), 491-505.